

**Detection Sensitivity Analysis for a Potential Drop (PD)
Structural Health Monitoring (SHM) System**

Seth S. Kessler and Christopher T. Dunn
Metis Design Corporation

Paul Swindell
FAA Technical Center

William Meeker
Iowa State University

IWSHM-2019

ABSTRACT

The paper presents a detection sensitivity analysis for a novel approach to monitoring fatigue crack growth. A carbon nanotube (CNT) sensor was used based on a potential drop (PD) damage detection strategy. Resistive CNT film was laminated between impermeable membranes to create a durable crack gauge that can resist high strain levels, high temperatures and submersion in water. Any crack growth below the sensor would disrupt the CNT electrical entanglement, therefore increasing the network resistance. As opposed to traditional crack gauges with discretized output based on broken copper traces, the CNT crack gauge provides for a continuous range of output, with resistance change proportional to the square of the crack length. The purpose of the present study was to evaluate the sensitivity of this CNT sensor to damage size using statistical approaches recently developed specifically to be applied to Structural Health Monitoring (SHM), including the Length at Detection (LaD) and REpeated Measured Random Effects Model (REM²) techniques.

INTRODUCTION

Probability of Detection (PoD) as defined in MIL-HDBK-1823A is typical used as the key metric to evaluate the risk involved when using specific non-destructive techniques to inspect structures. As Structural Health Monitoring (SHM) sensors are being considered to guide, supplement or replace strategic time-consuming inspections, a comparable metric must be produced to ensure risk levels are not increased. Following typical approaches for generating PoD can be quite costly for SHM sensors however, as they are permanently installed on the test structure thus requiring new sensors be used for each data point. Traditional PoD also does not allow for repeated inspections—observing a flaw at multiple points in time as it grows on the same structure—as it raises concern that not enough variability is captured. Therefore, new approaches have been proposed to assess the sensitivity of SHM methods for detecting damage that incorporates the statistics associated with repeated measurements, with the hope that in the near future these approaches will be validated to be comparable to traditional PoD.

Seth S. Kessler, Metis Design Corporation, Boston, MA 02114, USA
Christopher T. Dunn, Metis Design Corporation, Boston, MA 02114, USA
Paul Swindell, FAA Technical Center, Atlantic City, NJ 08405, USA
William Meeker, Iowa State University, Ames, IA 50011, USA

APPROACH

While more complex SHM methodologies have been demonstrated with various levels of success, great benefit could be realized by extremely simple “fuse-style” sensors. In its simplest embodiment, a fuse-style sensor could just be a single conductive trace with a binary response; either a crack has grown long enough to break electrical continuity or not. Multiple traces can be patterned to produce a pseudo-digital response. The present work investigates a continuum crack gauge fabricated using commercial CNT sheets embedded into a conformal sensor comprising of film adhesive and electrode layers. The CNT form a network resistance that increases with crack growth. Benefits over commercial foil gauges include better durability under static and fatigue loads, not being susceptible to corrosion, elimination of single-point-failures, and being able to be formed in any size or shape, including with cutouts.

MODELING

Using Ansys 18.1, a finite element model (FEM) of the CNT sensor with a crack was created changing electrode spacing and width, sheet resistance, and crack length. The FEM consisted of a of 4096 eight node plane230 elements with voltage degrees of freedom. The FEM analyzes half the geometry, with 0.5 V applied to nodes on the right-hand side of the model to form an electrode, and 0 V applied to some nodes of the left-hand side of the model as a symmetry boundary condition. The crack was modeled by removing some of these 0 V nodes. Figure 1 shows the FEM results and fit to the data.

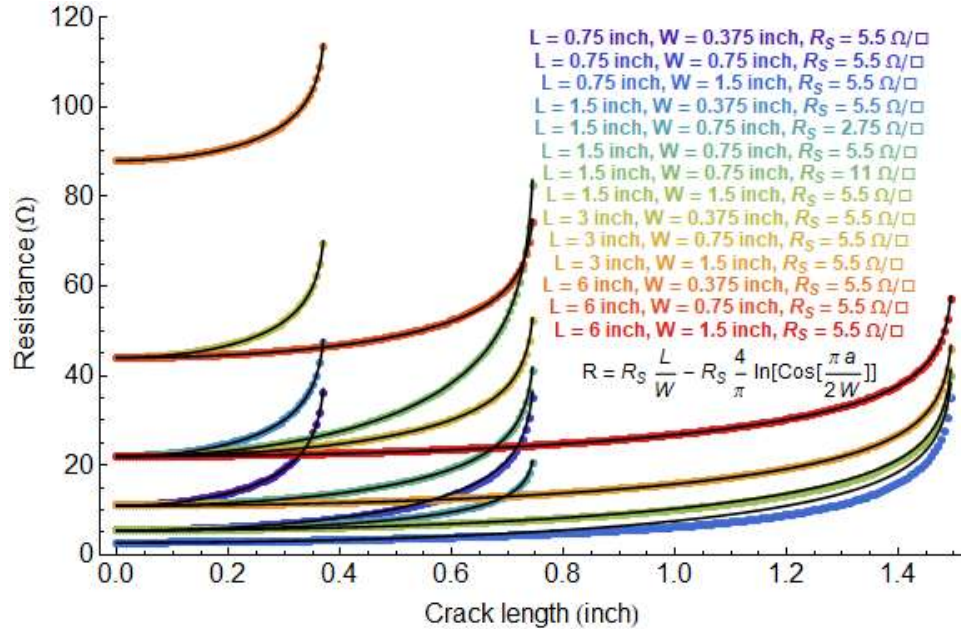


Figure 1. Finite element results plotting resistance versus crack length

As can be seen in Figure 1, the resistance can be fit as a function of crack length:

$$R = R_0 - R_S \frac{4}{\pi} \ln\left(\cos\left(\frac{\pi a}{2W}\right)\right) \quad \text{where } R_0 = R_S \frac{L}{W} \quad (1)$$

These equations work well as a fit to the results, except for values of $W / L > 2$, that is a wide sample but a narrow electrode spacing. For small crack lengths compared to the width Equation 1 is approximately given by:

$$R = R_0 + R_s \frac{\pi a^2}{2 w^2} \quad \text{small } a/w \quad (2)$$

Solving Equation 2 for crack length versus measured resistance yields:

$$a = \sqrt{\left(\frac{R}{R_0} - 1\right) \left(\frac{2 wL}{\pi}\right)} \quad \text{small } a/w \quad (3)$$

Inspecting Equation 3 shows that the estimated crack length is a function of the square root of normalized change in resistance from the initial value, times a “gauge factor” G_f that is dependent on sensor geometry.

$$a = G_f \sqrt{\Delta \bar{R}} \quad \text{small } a/w \quad (4)$$

$$\Delta \bar{R} = \left(\frac{R}{R_0} - 1\right) \quad \text{and} \quad G_f = \sqrt{\left(\frac{2 wL}{\pi}\right)} \quad (5)$$

PROOF OF CONCEPT EXPERIMENTAL SETUP

A 4-point bend fixture was used to grow a natural crack from a 1.5 mm EDM notch by applying an 80% yield load at 1 Hz to 300 x 25 x 3 mm aluminum bars. A digital microscope was used to capture truth data at ~1.5 micron resolution (16 pixels per 25 micron), and the entire setup was synchronized with LabVIEW, such that at pre-specified cycle numbers resistance data and an optical image could be captured.

A total of 19 identical specimen were cycled at room temperature for 20,000 cycles with CNT resistance being measured every 100 cycles in both the fully loaded and unloaded positions. Starting at 20,000 cycles, an image was captured every 1,000 cycles to capture the crack extending from the tip of the EDM notch (usually optically detectable around 25 micron between 22,000 and 28,000 cycles). Cycling would continue until 50,000 cycles which resulted in ~12 mm crack. Along with each resistance measurement, also collected were time, temperature, load, and the resistance of an unloaded witness specimen adjacent to the test setup. In addition to measurements in the fully loaded and unloaded positions, for one specimen, data was also collected at 1/3 and 2/3 of full load to explicitly determine the effect of strain on sensor response. Finally, 6 of the specimens were further tested at elevated or reduced temperatures. Here, when cycling was paused for imaging, the specimen would be heated or cooled for 10 minutes—with data collected once a minute—to capture the effect of temperature on the resistance measurements. For elevating the temperature, a space heater was used to raise the specimen temperature up to 40°C. For reducing the temperature, a thermoelectric Peltier cooler was used to lower the specimen temperature down to 0°C.

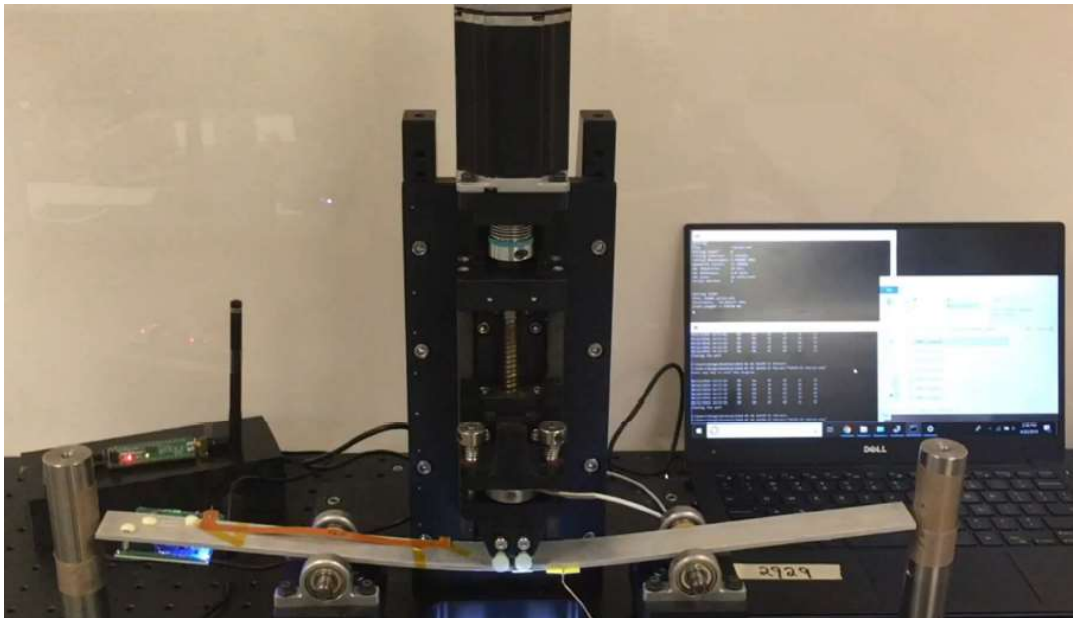


Figure 2. 4-point fatigue bend test fixture

PROOF OF CONCEPT EXPERIMENTAL RESULTS

Using equations 4 and 5, the crack length could be predicted for a given value of R . As calculated, G_f had a value of 20.86 for width $w = 18$ mm and length $L = 38$ mm. However, running an optimization to minimize the prediction error yielded an effective G_f of 19.86; since these values were within 5%, a round value of 20 mm was used. A threshold value of 0.1% was used for $\Delta\bar{R}_T$ based on the measured noise floor, meaning the minimum detectable crack size was forced to ~ 0.625 mm. Figure 3 shows all of the predicted crack length data for all specimens, plotted against the optically measured crack length. The dotted black line represents a slope of 1 ($y = x$) which would be the ideal prediction values. It can be seen that all the data closely adheres to the ideal value, with just a few outliers that overpredict crack size for large true crack lengths. Figure 4 is a zoomed-in view of Figure 3, focusing on the initial 2 mm of crack length.

Two approaches were taken to determine SHM system detection sensitivity by Prof. Bill Meeker at Iowa State University. Figure 5 shows the Gaussian distribution results of the Length at Detection (LaD) method for computing detection sensitivity. According to this analysis, which just considers data up until the threshold crossing values, the $a_{90/95}$ value is 1.3 mm, seen in Figure 6. Next, density plots of Bayesian estimation were calculated to calculate detection sensitivity using the REpeated Measures Random Effects Model (REM²). Here, points before and after detection and used to determine damage index slopes and explicitly account for repeated inspections statistically. Of particular note, the mean value of μ beta (mean slope) is 0.99, which means that the selected value of G_f provided an excellent fit. Also of note is the value standard deviation of 0.023, which means the results have a 2σ of $\pm 5\%$ on the crack size predictions. Figure 6 shows an $a_{90/95}$ value of 1 mm using data up to 5 mm crack length, however that value ranged as high as 1.3 mm using all the collected data to as low as 0.94 mm using data just up until 2 mm. Higher error at larger crack lengths tended to more dramatically affect the slope for this statistical approach.

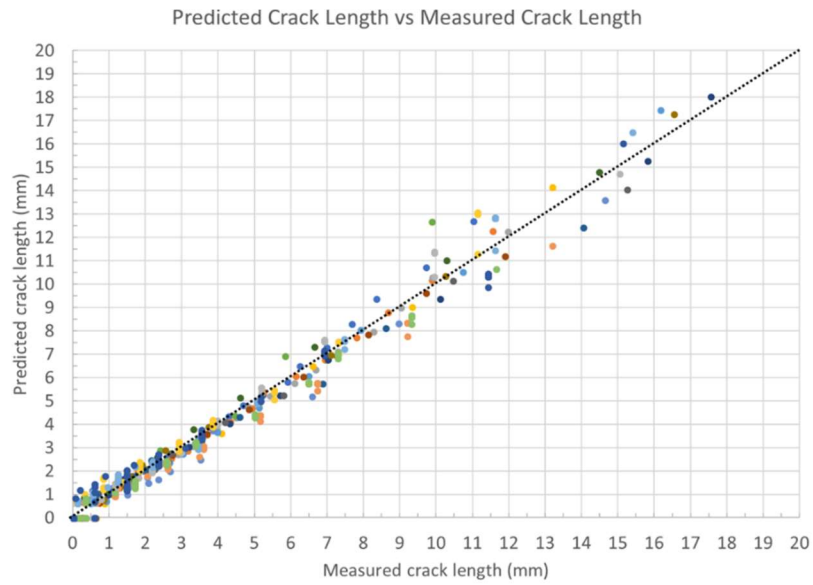


Figure 3. Predicted crack vs measured crack length for all specimens at all temperature ranges

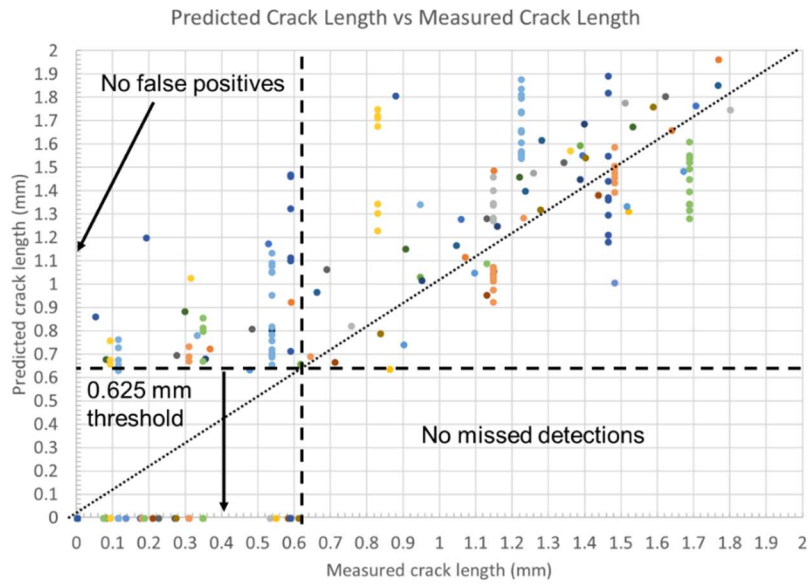


Figure 4. Zoomed predicted crack vs measured crack length for all specimens at all temperature ranges

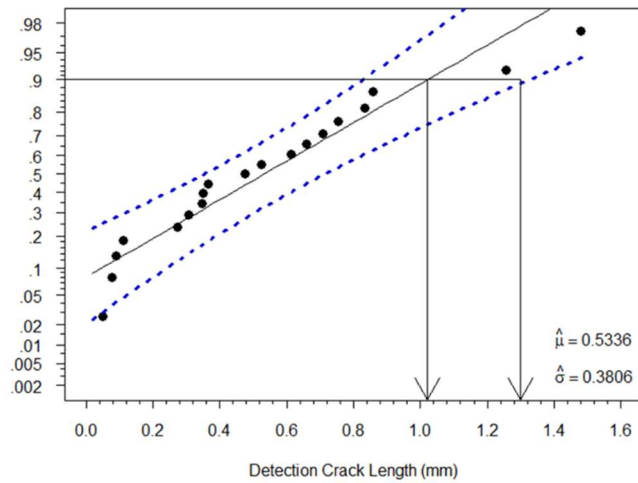


Figure 5. Gaussian distribution probability plot for LaD approach

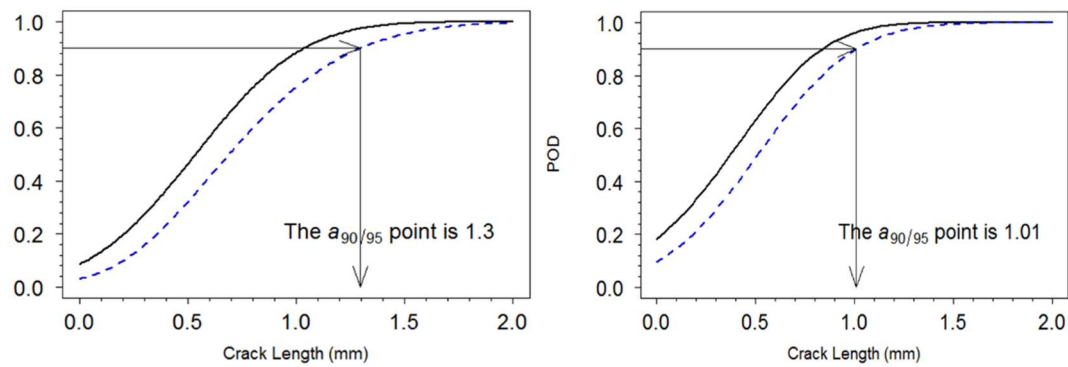


Figure 6. Detection sensitivity estimate using LaD approach (left) and REM² approach (right)

BLIND VALIDATION EXPERIMENTAL SETUP

In collaboration with the FAA William J. Hughes Technical Center, a series of fatigue tests were performed to further evaluate the two detection sensitivity statistical approaches being evaluated. A dozen 600 x 40 x 2 mm specimens were water-jet cut from a large plate of Aluminum-Lithium alloy provided by the FAA, as seen in Figure 7. A 5 mm edge notch was electrical-discharge machined (EDM) into each following ASTM E647. Sacrificial specimens of similar dimensions were used by the FAA to determine the appropriate load, load rate, and approximate cycles to initiation and failure. Each specimens were instrumented with a 22 x 22 mm CNT crack gauge bonded to the middle of the bar, offset ~1 mm from the EDM notch. PZT sensors were also bonded on either side of the crack gauge to collect ultrasonic data for the same specimens, however this data is presented in a separate paper.

Subsequently, natural fatigue cracks were grown through 35,000 tension-tension cycles, representing up to ~9 mm of crack growth, with data being collected every 1,000 cycles. Data was collected wirelessly using a radio frequency harvesting antenna designed by Analog Devices, and was processed using Equations 4 and 5 to estimate crack length. A total of 12 specimens were tested, however three of the specimens were improperly soldered by the FAA and yielded invalid data, thus were excluded from this study. True crack data was only provided for a single specimen for calibration purposes, and the rest of the data was processed blindly with only resistance versus cycle data.



Figure 7. Al-Li tensile-fatigue specimens instrumented with CNT crack gauges (left). MTS setup for fatigue crack growth and optical measurement of actual crack length (right)

BLIND VALIDATION EXPERIMENTAL RESULTS

Figure 8 plots the predicted crack length based on the CNT sensor output versus the actual measured crack length for all specimens (similar to Figure 3 but much less data). Again, the predicted crack length was solely based on Equations 4 and 5, slightly increasing the G_f value to 18 mm (from the calculated value of 17.55) to best fit the calibration specimen. Truth data was measured optically, and was provided after crack predictions versus cycle count had already been submitted to the FAA. Subsequently, the blind results along with the true crack data was provide to Prof. Bill Meeker at Iowa State University to evaluate using the LaD and REM² approaches. As seen in Figure 9, these analysis resulted in $a_{90/95}$ values of 2.9 mm for both statistical models.

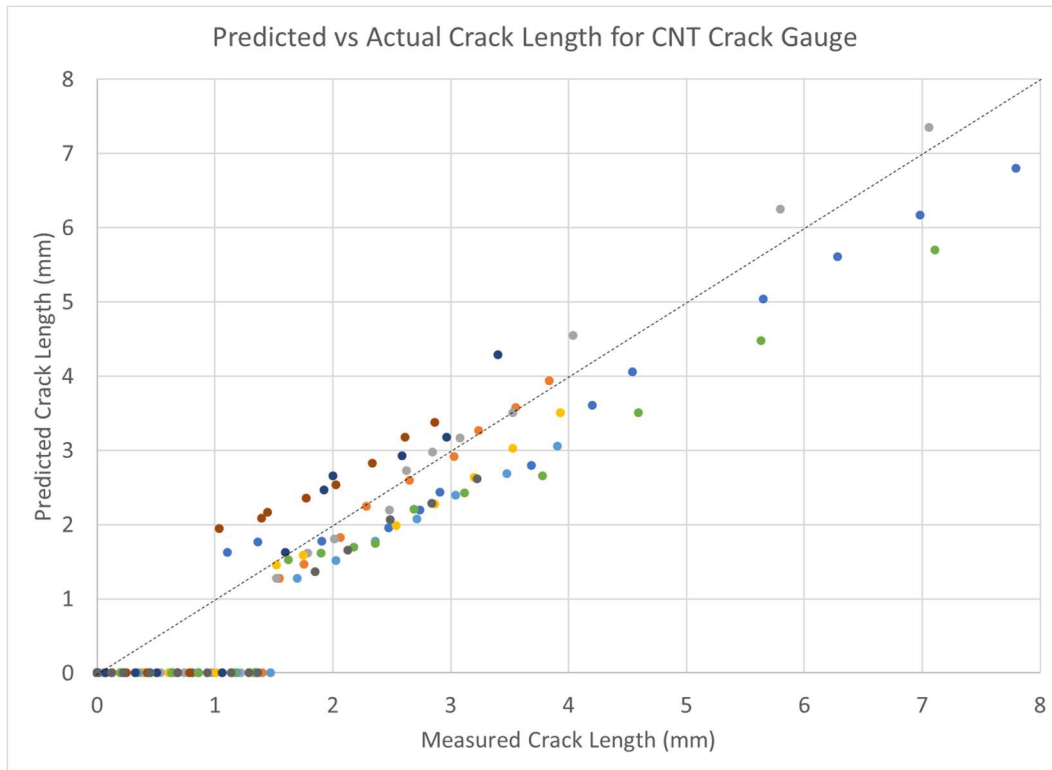


Figure 8. Predicted crack vs measured crack length for all specimens

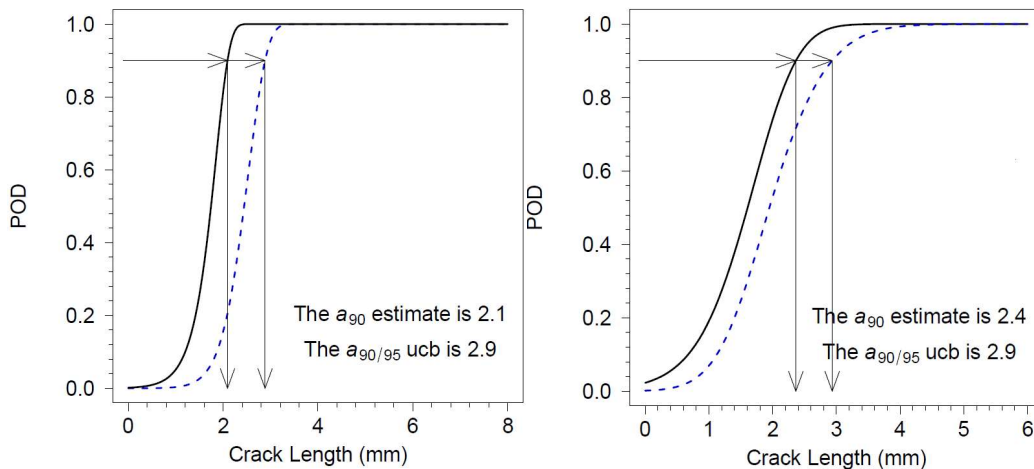


Figure 9. Detection sensitivity estimate using LaD approach (left) and REM² approach (right)

CONCLUSIONS

This paper presents a simple passive potential drop approach to monitoring fatigue cracks using CNT-based sensors. The sensor is bonded to a structure similar to a strain gauge or conventional foil crack gauge, and the CNT sheet forms sheet resistance that increases as a crack grows across the sensor, and increases the effective current path between electrodes. A FEM was built to predict sensor behavior, which was fit into a simple equation that relates crack length to the square root of resistance change. A series of 19 specimen were tested in 4-point bend fatigue to demonstrate the principal, including variations in temperature and strain at the time of data recording. These results showed reliable detection of cracks ~1 mm in length. A second test was conducted blindly with the FAA on 9 specimens, which similarly showed sensitivity of ~3 mm for natural cracks growing from EDM notches in tensile-tensile fatigue specimens. It is believed that the blind experiment yielded a lower sensitivity due to additional heating of the specimens during tensile fatigue, as well as the much smaller sample set size. For both sets of tests, statistical analysis was performed using the newly formulated LaD and REM² approach to determine detection sensitivity as a proposed alternative to PoD formulation via MIL-HDBK-1823A. In the future, we plan to collect a much larger set of data in order to further validate these proposed detection sensitivity models.

ACKNOWLEDGMENTS

This research was performed at the Metis Design Corporation in Boston, MA, and the FAA Technical Center Atlantic City, NJ, sponsored by the USAF under SBIR contract FA8650-15-C-2563 and by the FAA under ANG-TT-CRDA-0352.

REFERENCES

1. Raghavan A., Kessler S.S., Dunn C.T., Barber D., Wicks S. and B.L. Wardle. "Structural Health Monitoring using Carbon Nanotube (CNT) Enhanced Composites." Proceedings of the 7th International Workshop on Structural Health Monitoring, 9-11 September 2009, Stanford University.
2. Wicks S., Barber D., Raghavan A., Dunn C.T., Daniel L., Kessler S.S. and B.L. Wardle. "Health Monitoring of Carbon NanoTube (CNT) Hybrid Advanced Composite for Space Applications." Proceedings of the 11th European Conference on Spacecraft Structures, September 2009 Toulouse, France.
3. Barber D., Wicks S., Wardle B.L., Raghavan A., Dunn C.T. and S.S. Kessler. "Health Monitoring of CNT Enhanced Composites." Proceedings of the SAMPE Fall Technical Conference, October 2009, Wichita, KS.
4. Kessler S.S., Raghavan A., Dunn C.T., Wicks S., Guzman deVilloria R., and B.L. Wardle "Fabrication of a Multi-Physics Integral Structural Diagnostic System Utilizing Nano-Engineered Materials." Proceedings of the 2nd Annual Conference of the Prognostics and Health Management Society, October 2010, Portland, OR.
5. Guzman de Villoria, R., Kessler, S.S., Yamamoto, N., Miravete, A., and B.L. Wardle. "Multi-Physics Nano-engineered Structural Damage Detection and De-icing." Proceedings of the 18th International Conference on Composite Materials, 21-26 August 2011, South Korea.
6. Kessler S.S., Dunn C.T., Wicks S., Guzman deVilloria R. and B.L. Wardle. "Carbon Nanotube (CNT) Enhancements for Aerosurface State Awareness." Proceedings of the 8th International Workshop on Structural Health Monitoring, 12-15 September 2011, Stanford University.
7. Guzmán de Villoria, R., Yamamoto, N., Miravete, A., and B.L. Wardle, "Multi-Physics Damage Sensing in Nano-Engineered Structural Materials," online in *Nanotechnology*, April 2011.
8. Kessler S.S., Thomas G., Borgen M. and C.T. Dunn. "Performance Analysis for CNT-based SHM Composite Structures." Proceedings of the 9th Int'l Workshop on SHM, September 2013, Stanford University.
9. Kessler S.S., Thomas G., Borgen M. and C.T. Dunn. "Carbon Nanotube Appliques for Fatigue Crack Diagnostics." Proceedings of the 10th Int'l Workshop on SHM, September 2015, Stanford University.
10. Kessler S.S. and C.T. Dunn "Reliability Assessment for NanoEngineered Fatigue Crack Sensor." Proceedings of the 11th International Workshop on Structural Health Monitoring, 12-14 September 2017, Stanford University.